EPR Kinetic Studies of Oxygen Release in Thylakoids and PSII Membranes: A Kinetic Intermediate in the S_3 to S_0 Transition†

M. Reza Razeghifard‡ and Ronald J. Pace*

Department of Chemistry, Faculty of Science, The Australian National University, Canberra, Australia 0200

Received May 18, 1998; Revised Manuscript Received October 12, 1998

ABSTRACT: Time-resolved EPR oximetry has been used to determine the oxygen release kinetics in spinach thylakoids and PSII membranes. We observe release kinetics with half-times of ∼0.85 and ∼1.45 ms for thylakoids and PSII membranes, respectively, which are in close agreement with the EPR determined Y_z decay kinetics for the $S_3 \rightarrow \rightarrow S_0$ transition in these systems. The results show conclusively that water-oxygen chemistry is not a rate-limiting step in the donor side of PSII under normal turnover conditions. By analyzing the oxygen release kinetics in thylakoids under nonphysiological, but still functionally competent conditions (low pH or high salt), we observed an initial delay in the O_2 release of up to 200 μs following flash turnover from the S_3 state. This is the first direct indication of a probable quasi-stable intermediate in the $S_3 \rightarrow \rightarrow S_0$ turnover of PSII, possibly representing the putative S_4 state. Under conditions more closely approaching physiological, no such delay was resolved, indicating that the $S_4 \rightarrow O_2$ transition occurs within 50 μs under such circumstances. Two possible reaction sequences for O_2 formation consistent with these and other data are discussed. It is suggested that the more probable form of "S_4" is in fact the $S_3 + Y_z^{\bullet}$ combination, which must undergo some molecular rearrangement on the tens to hundreds of microseconds time scale before O_2 formation chemistry occurs.

In oxygenic photosynthetic organisms, water is oxidized to molecular oxygen by a manganese-containing catalytic site in Photosystem II (PSII),[1] which involves up to four Mn ions. The four required oxidizing equivalents for the water oxidation are sequentially accumulated in the Mn cluster by changing its redox state. The formal redox states of the Mn cluster are known as the S states, labeled S_0-S_4, where the index represents the number of oxidizing equivalents stored (*1*). The S_4 state is unstable, and its spontaneous reduction to S_0 is accompanied by oxygen release. A tyrosine residue, Y_z, is an intermediate electron carrier which transfers the oxidizing equivalents from $P680^+$ to the Mn cluster (*2, 3*). Since the rate of $Y_z^{\bullet}$ rereduction is S-state-dependent, the time scale of each $S_i \rightarrow S_{i+1}$ transition can be obtained by measuring the $Y_z^{\bullet}$ rereduction kinetics. In intact systems the EPR signal of $Y_z^{\bullet}$ (neutral radical) is conventionally called signal II_{vf} (*4*). The first determinations of these kinetics by the observation of EPR transients of $Y_z^{\bullet}$ were performed by Babcock and co-workers (*5*). Recently, we have refined this technique and provided a detailed description of the S state turnover kinetics by EPR for the four meta stable S states, S_0 to S_3 (*6, 7*). The uncertainties in the time constants associated with these transitions are now only a few tens of microseconds.

It has for some time been realized that the time scale for flash-induced oxygen release in the $S_3 \rightarrow (S_4) \rightarrow S_0$ transition is of an order similar (one to a few milliseconds) to that of the S_3 state turnover, with the latter monitored by EPR or optical absorption techniques (for a summary see ref *6*). Generally, however, the time resolution of the oxygen release measurements has been significantly poorer than that of the S_3 turnover determinations, with the result that only a coarse upper limit could be put on the lifetime of the putative S_4 state. Oxygen formation kinetics have been studied in a number of different ways, with the apparent oxygen release times being shown to depend on the technique and the material used. Using polarographic techniques the half-time of oxygen release was estimated as about 0.9 ms (*8*), 2 ms (*9*), and 1.5−2.2 ms (*10*) in *Chlorella*; 3 ms (*11*) and 1.2 ms (*12*) in chloroplasts; 2.7 ms or <6 ms (*13*) in thylakoids; <5 ms (*13*) and 30−130 ms (*14*) in PSII membrane fragments; <11 ms (*13*) in leaf disks; and 1.2 ms (*15*) in *Dunaliella tetiolecta*. The half-time of oxygen release was also shown to be less than 5 ms (ref *16* and see also ref *17*) in leaf disks using the photoacoustic technique and 3 ms using a UV absorption spectroscopy technique (*18*).

The fact that the lower limit of these various estimates (millisecond time scale) overlaps with the observed range for S_3 state turnover in thylakoids or PSII membrane fragments (0.75 or 1.4 ms, see refs *6, 7*) has supported the view that the water oxygen chemistry is not the rate-limiting step in the electron donor side of PSII, although this idea has been challenged (*14*). However the data at present are of insufficient precision to resolve the issue, and derive in general from measurements made on different systems under not necessarily comparable conditions.

† This work was supported by the Australian Research Council. M.R.R. is in receipt of a MCHE scholarship.

* To whom correspondence should be addressed.

‡ Current address: Department of Biochemistry, University of Minnesota, St Paul, Minnesota 55108. Fax: (+61)-2-6279-8997. E-mail: Ron.Pace@anu.edu.au.

[1] Abbreviations: EPR, electron paramagnetic resonance; HEPES, *N*-2-hydroxyethyl piperazine-*N*′-*2*-ethanesulfonic acid; PBQ, paraben-zoquinone; PPBQ, phenyl-*p*-benzoquinone; PDT, ^{15}N-perdeuterated tempone; PSII, Photosystem II.

10.1021/bi9811765 CCC: $18.00
Published on Web 01/05/1999

The oxygen release time has been recently measured using an alternative approach (*19, 20*). This technique, EPR oximetry, is based on the effect of molecular oxygen, as a paramagnetic species, on the EPR spectra of stable radicals. Through paramagnetic spin−spin interaction, collisions between molecular oxygen and the spin probe will result in changes in the spectrum line width and microwave saturation behavior of the spin probe, due to effects on both the T_1 and T_2 relaxation times of the probe. At high microwave power levels, an increase in the oxygen concentration causes a proportional increase in the peak height of the oxygen probe (*7*).

In comparison with the polarography technique, EPR oximetry has one major disadvantage, its poor signal-to-noise ratio, especially in time-resolved EPR oximetry. However if this limitation can be accommodated, EPR oximetry has numerous advantages as a technique for determining rapid changes in dissolved oxygen concentrations. The measurement is truly "in situ", with negligible time lags associated with mixing or boundary layer diffusion processes. In addition, oxygen is not consumed by the measurement, nor are reactive species such as H_2O_2 formed.

By using ^{15}N-perdeutrated Tempone as the oxygen probe, Strzalka et al. (1990) reported a half-time of 0.4−0.5 ms for the oxygen release time in spinach thylakoids, which unexpectedly, was faster than any previously reported half-time for the $S_3 \rightarrow S_0$ transition. However, by using lithium phthalocyanine as the oxygen probe (*19*), Tang et al. measured a half-time of 1−2 ms for oxygen release time in PSII membranes, which is in closer agreement with oxygen electrode measurements.

In this paper we report the oxygen release kinetics from PSII obtained from extensive averaging of the flash-induced change in the signal amplitude of PDT, using time-resolved EPR oximetry. We have also measured the signal II_{vf} kinetics of the sample under the same experimental conditions as were used for the oxygen release kinetics. This allows, for the first time, a direct comparison of the $S_3 \rightarrow S_0$ transition kinetics with the oxygen release kinetics in the same photosynthetic system. Comparison of the data of thylakoids under physiological conditions (pH 7.5) with those under nonphysiological conditions (low pH and high salt) shows the presence of a resolved intermediate in the $S_3 \rightarrow S_0$ transition. Also, it is clearly shown that oxygen release is retarded in detergent-solubilized PSII membrane particles, in comparison with thylakoids as active physiological samples.

MATERIALS AND METHODS

Thylakoid membranes were isolated from market spinach. About 400 g of leaves were deveined and homogenized in 50 mM HEPES/NaOH (pH 7.5), 5 mM $MgCl_2$, 50 mM NaCl, and 0.4 M sucrose. The homogenate was strained through 8 layers of cheesecloth and one layer of nylonmesh (35 μm) and centrifuged at 1000*g* for 10 min. The pellet was resuspended in 50 mM HEPES/NaOH (pH 7.5), 5 mM $MgCl_2$, and 50 mM NaCl to give an osmotic shock and centrifuged at 1500*g* for 10 min. The pellet was finally resuspended in the homogenizing buffer as buffer A, in 50 mM HEPES/NaOH (pH 7.5), 5 mM $MgCl_2$, 3 mM $CaCl_2$, and 0.8 M NaCl as buffer B, or in 50 mM MES/NaOH (pH 6.0), 5 mM $MgCl_2$, 50 mM NaCl, 3 mM $CaCl_2$, and 0.4 M sucrose as buffer C. The chlorophyll concentration was adjusted to 2 mg/mL. PSII membranes were prepared as previously described (*7*). The final pellet of PSII membranes was resuspended in 50 mM MES/NaOH (pH 6.0), 5 mM $MgCl_2$, 15 mM NaCl, 3 mM $CaCl_2$, and 0.4 M sucrose as buffer D. The chlorophyll concentration was adjusted to 2 mg/mL. All preparation steps were performed at 4 °C in dim light, and the chlorophyll concentration was determined by the method of Porra et al. (*21*).

The O_2 evolution activity was measured with a Clark-type electrode. For thylakoids the O_2 activity was measured in the assay mixture of buffer A, B or C containing 0.25 mM PPBQ, 0.5 mM ferricyanide, and 5 mM NH_4Cl. For PSII membranes the O_2 activity was measured in 50 mM MES/NaOH (pH 6.0), 5 mM $MgCl_2$, 15 mM NaCl, 3 mM $CaCl_2$, 0.4 M sucrose, 0.25 mM PPBQ, and 0.5 mM ferricyanide as the assay mixture. The chlorophyll concentration during the assay was about 20 μg/mL. The steady-state rates of oxygen evolution for thylakoids and PSII membranes were typically between 220 and 260 or 450 and 500 μmol of O_2 (mg of Chl)$^{-1}$ h^{-1}, respectively. These did not decline by more than 15% between the beginning and end of a kinetic run.

All EPR measurements were carried out at 8−10 °C on a Bruker ESP 300E spectrometer equipped with a TM011 cavity. The sample was continuously pumped (∼30 μL/s) through the EPR cuvette from a long tube, functioning as a reservoir and kept in a water bath at 4 °C in the dark. Saturating 10 μs xenon flashes from an EG&G electrooptics flash lamp were used to excite the sample. A fiber optic cable was used as a light guide to illuminate the sample directly in the EPR cavity. The flash frequency (4 Hz) and pump flow rate were chosen to allow each aliquot to receive <15 flashes within the EPR cavity. This is critical because excessive turnover on any aliquot leads to slight signal position drift, which distorts the kinetic output. A data run consisted of 5000−10000 flashes in total.

^{15}N-perdeutrated tempone (PDT) (from C/D/N isotopes Quebec, Canada) was used as an oxygen probe to measure the O_2 release kinetics (see ref *20*), at a final concentration in the sample of 100 μM.

The signal II_{vf} kinetic measurements were performed using 100 kHz modulation frequency, 100 mW microwave power, 4 G modulation amplitude, and 40 μs time constant, at the low-field peak of signal II_s ($g = 2.010$). PBQ 1 mM and 1 mM $K_3Fe(CN)_6$ or 1 mM PPBQ and 1 mM $K_3Fe(CN)_6$ were included as the electron acceptors for thylakoids and PSII membranes, respectively. A field-independent flash artifact was measured at a position 50 G offset from $g = 2.00$ and subtracted from the signal II kinetic signals (*6, 7*)

The oxygen release measurements were performed using 100 kHz modulation frequency, 159 mW microwave power, 2.5 G modulation amplitude, and 160 or 320 μs time constant. The measurement position was at the downfield peak of the PDT signal, in the presence of the above artificial electron acceptors. We have shown earlier (*7*) that under these conditions of saturating power and overmodulation, the signal peak to peak amplitude increases monotonically with dissolved O_2 concentration. The PDT peak is centered

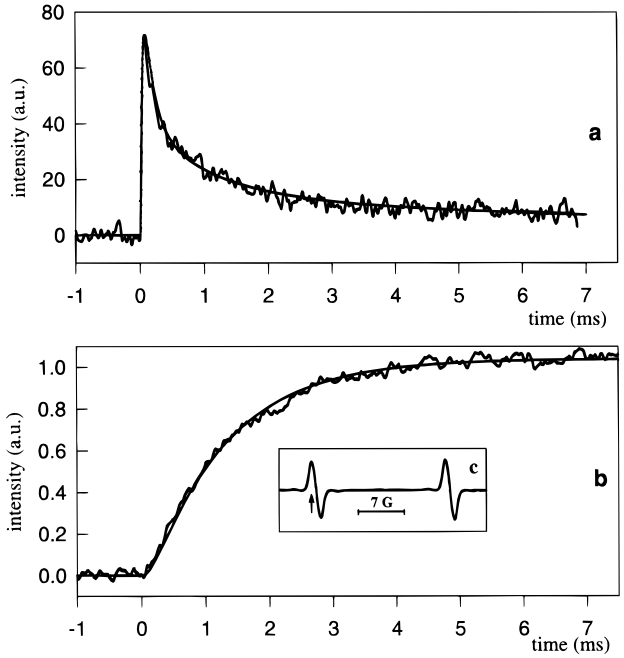

FIGURE 1: (a) The signal II_{vf} kinetics and fit of eqs 3 and 4 plus (b) the oxygen release kinetics and fit of eqs 1 and 2 for repetitive flashing on a sample of dark-adapted thylakoids in buffer A (pH 7.5). The signal amplitudes are divided by the number of averaged events: 18 000 for the signal II_{vf} kinetics and 40 000 for the oxygen release kinetics. The insert to panel (b) shows the PDT spectrum and peak used for the measurement. The instrument time constant for oxygen release measurements is 160 μs. Other conditions are as described in Materials and Methods.

at $g = 2.015$ and overlaps the signal II measurement point somewhat. However the signal, due to the probe concentration and narrow line width, is ~100 times more intense than signal II components.

Timing and control of the EPR acquisition were performed by the ESP 300E spectrometer computer. During acquisition of a kinetic signal, the flash lamp was triggered after a (short) fixed delay in the acquisition sequence, to obtain data both immediately before and after the flash.

RESULTS

Figures 1, 2, 3, and 4b show the oxygen release kinetics measured by monitoring changes in the signal amplitude of the PDT signal. The data were obtained by subtracting the kinetic traces measured at the positive peak of the PDT signal from the corresponding traces measured at its negative peak (Figure 1b, insert). This improves the signal-to-noise ratio and cancels any background signals arising from flash artifacts or signal II turnover. The sample was circulated continuously, and each dark-adapted aliquot received about 12 flashes. During the course of the kinetic measurements the PDT spectrum was regularly scanned and the magnetic field periodically readjusted to maintain position on the PDT measurement peak. This procedure is necessary as cavity tuning varies slightly throughout the course of the measurements, due to dissolved O_2 accumulation in the sample,-among other factors.

For the $S_3 \rightarrow (S_4) \rightarrow O_2$ transition, the response of the PDT probe to the turnover-induced dissolved oxygen change can be defined by the following equations.

Table 1: Results of S_3 Kinetic Turnover Measured by Signal II_{vf} Rereduction and Oxygen Release, Determined by Time-Resolved EPR Oximetry[a]

	signal II_{vf} kinetics	oxygen release kinetics		
	$S_3 \rightarrow S_4$ $t_{1/2}$ (ms) a	$S_3 \rightarrow S_0$ $t_{1/2}$ (ms) b	$S_3 \rightarrow S_4$ $t_{1/2}$ (ms) c	$S_4 \rightarrow S_0$ $t_{1/2}$ (ms) d
thylakoids (pH = 7.5)	0.75	0.85	0.80	<0.05
thylakoids (pH = 6.0)	1.05	1.25	1.05	0.2
thylakoids (0.8 M NaCl)	1.3	1.4	1.3	0.1
PSII membranes	1.4	1.4	1.45	<0.05

[a] Interpretation of parameters according to Scheme 1 (See text). The O_2 kinetics show half-times for the overall release process (b, not generally simple exponential) and its decomposition into sequential first-order processes (c, d), according to reactions in Scheme 1. The uncertainty (from data fits) for a, b, and c is ~5% and for d is ~20%.

For $t < 0$

$$A_{(t)} = 0 \tag{1}$$

for $t > 0$

$$A_{(t)} = [S_3]\left(1 + \frac{k_1 e^{-k_2 t} - k_2 e^{-k_1 t}}{k_2 - k_1}\right) \tag{2}$$

where k_1 is the rate constant for the $S_3 \rightarrow S_4$ transition and k_2 is the rate constant for the spontaneous transition of $S_4 \rightarrow O_2$. A_t is the amplitude of the PDT signal at time t and [S_3] the fractional S_3 state population immediately before the flash. The smooth curves in Figures 1, 2, 3, and 4b represent the least-squares fits of the above equations, including the instrument response time, to the experimental data points. The resulting oxygen release half-times are listed in Table 1.

Figures 1a, 2a, 3a, and 4a show the signal II_{vf} kinetics obtained by repetitive flashing of a sample aliquot, summed over many aliquots. The Y_z kinetic signals were obtained under the same conditions as those used for oxygen release measurements, except that the PDT probe was absent. The response should correspond closely to that from a uniform mixture of the four S states. The smooth curves in Figures 1a, 2a, 3a, and 4a then represent the least-squares fits to the data of eqs 3 and 4, where for $t < 0$

$$I_{(t)} = 0 \tag{3}$$

for $t > 0$

$$I_{(t)} = I_a[0.75((e^{(-t/\tau_e)} - e^{(-t/\tau_r)})/(1/\tau_r - 1/\tau_e)) + 0.25((e^{(-t/\tau_f)} - e^{(-t/\tau_r)})/(1/\tau_r - 1/\tau_f))] + I_s[(e^{(-t/\tau_s)} - e^{(-t/\tau_r)})/(1/\tau_r - 1/\tau_s)] \tag{4}$$

where τ_f is the decay time constant for the turnover from S_3, τ_e is the average decay time constant for the three earlier S state transitions, τ_s is the decay time constant for turnovers of inactive centers, and τ_r is the instrument response time. I_a and I_s are the signal amplitudes for active and inactive centers, respectively, and are assumed to be S-state-independent. I_s corresponds to the fraction (10−15%) of nonfunctional centers which turnover with a decay time constant (τ_s) of ~10 ms. We have shown previously (*6*, *7*)

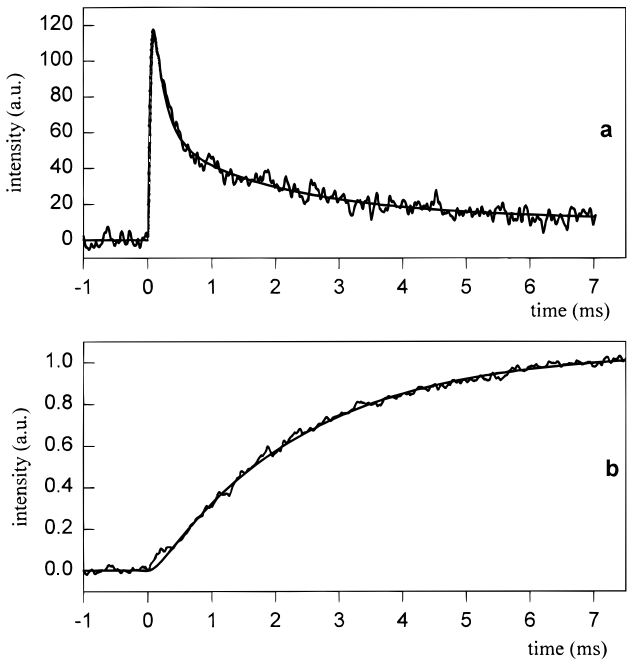

FIGURE 2: (a) The signal II_{vf} kinetics and (b) the oxygen release kinetics, with fits as in Figure 1, from repetitive flashing on a sample of dark-adapted PSII membranes in buffer D (pH 6.0). The signal amplitudes are divided by the number of averaged events: 20 000 for the signal II_{vf} kinetics and 40 000 for the oxygen release kinetics. Other conditions are as in Figure 1.

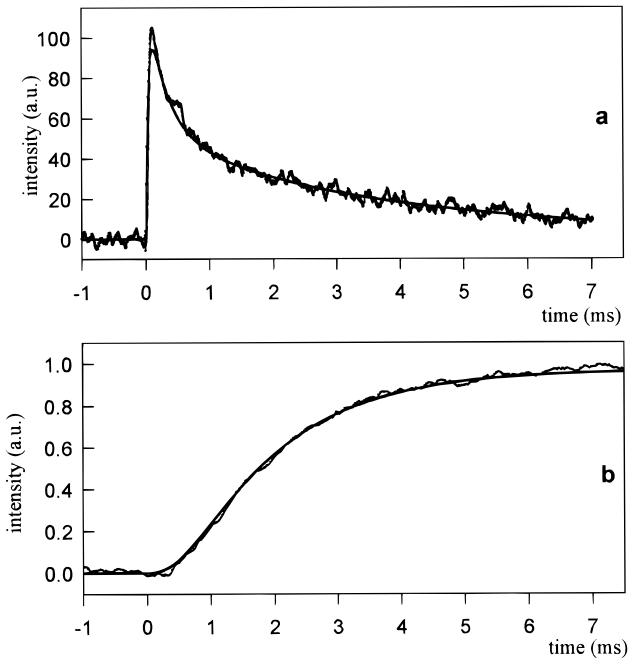

FIGURE 3: (a) The signal II_{vf} kinetics and (b) the oxygen release kinetics, with fits as in Figure 1, from repetitive flashing on a sample of dark-adapted thylakoids in buffer C (pH 6.0). The signal amplitudes are divided by the number of averaged events: 24 000 for the signal II_{vf} kinetics and 50 000 for the oxygen release kinetics. The instrument time constant for oxygen release kinetics is 320 μs. Other conditions are as in Figure 1.

that the decay time constants for the three early S state transitions in functional PSII centers are comparable, and differ by approximately an order of magnitude from that of the (slower) $S_3 \rightarrow \rightarrow S_0$ transition. This allows the latter to be isolated from a three exponential fit to the decay kinetics of unsynchronized sample turnovers. It is further assumed that the rise and fall kinetics of the $Y_z^\bullet$ signal in each S state are monoexponential, with the rise time governed by the spectrometer response (40 μs). The resulting half-decay times for $Y_z^\bullet$ rereduction following turnover from S_3 (listed as $S_3 \rightarrow S_4$), are given in Table 1.

Examination of Table 1 shows that, under conventionally optimal sample conditions (thylakoids at pH 7.5, PSII membranes at pH 6.0), the kinetics of signal II_{vf} decay and oxygen release match very closely. This clearly indicates that, under physiological (or near) conditions, photosynthesis is not rate-limited by the oxygen formation chemistry. The maximum delay we could infer between $Y_z^\bullet$ reduction and O_2 release is 50 μs, and the fits in Figures 1 and 2b) were made with this value. As we have previously reported (*6*, *7*), $Y_z^\bullet$ rereduction on the $S_3 \rightarrow (S_4) \rightarrow$ transition is significantly slower in PSII membranes than intact thylakoid preparations, although no comparable effect on the oxygen chemistry kinetics is resolvable in PSII. To determine if the $Y_z^\bullet$ reduction and O_2 release time scales could be separated, we sought to displace the system away from its physiological optimum. Our flexibility in this regard was limited, as the perturbed sample system still had to be stably functional over ~2 h for the EPR measurements. For this reason only thylakoids were examined. Two protocols were employed: lowering the external pH to 6.0 and suspending the thylakoids in high monovalent salt (0.8 M NaCl). Although the precise lumenal conditions obtained during turnover in these cases are not completely defined, qualitatively one may say that in the first instance the lumenal pH is ~5 and in the second the lumenal ionic strength is ~1 M. Both of these conditions are known to reversibly inhibit O_2 evolution and significantly perturb Y_z function in isolated PSII particles or core preparations (*22*, *23*). Their effects in the present instance were less severe, with near control levels of O_2 release per flash turnover being retained, as well as near normal S state cycling of Y_z.

Figure 3 shows the results for signal II_{vf} reduction and O_2 release kinetics for thylakoids in external pH 6.0 buffer. Although the principle kinetics for O_2 release again match closely that of Y_z reduction (Table 1) there is now a readily discernible lag of 200 μs in O_2 release, following flash turnover. The delay cannot be associated with the $Y_z^\bullet$ rise time, which in our hands is instrument response time-limited. Here this is 40 μs, but earlier work has shown (*22*, *24*, *25*) that Y_z oxidation, even in NaCl- or pH-inhibited samples, occurs within a few microseconds. The most detailed results of pH effects on Y_z, P_{680} kinetics have been summarized recently by Junge and co-workers (*23*).

Figure 4 shows the corresponding data for thylakoids in high salt. This reveals qualitatively the same pattern as in Figure 3, with a discernible initial lag in the O_2 release pattern, which then closely matches the kinetics of Y_z rereduction. The lag here (100 μs) is less than that observed by the low pH treatment, but the inhibition of the Y_z rereduction rate is somewhat greater. In fact, Table 1 shows that, in all cases examined here, the $Y_z^\bullet$ and usually the O_2 lag kinetics are slowed under nonphysiological approximating (thylakoids pH 7.5) conditions, but that there is no obvious correlation between the extent of these two effects.

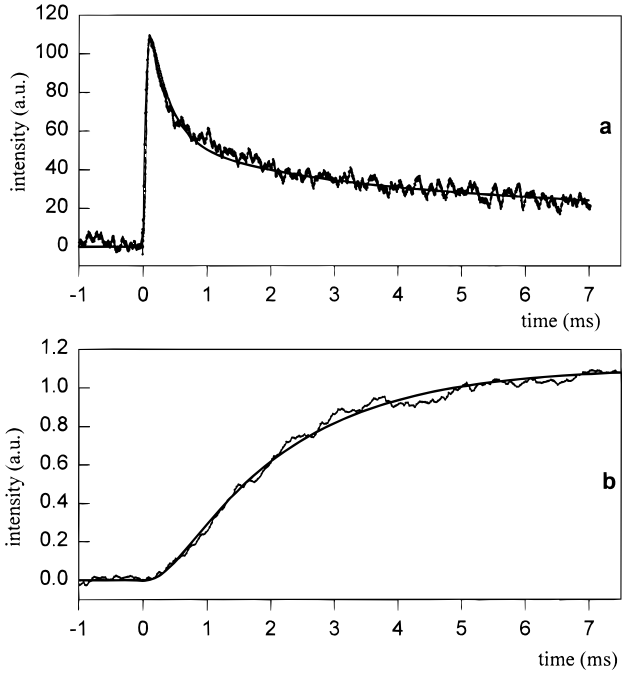

FIGURE 4: (a) The signal II_{vf} kinetics and (b) the oxygen release kinetics, with fits as in Figure 1, from repetitive flashing on a sample of dark-adapted thylakoids in buffer B (0.8 M NaCl). The signal amplitudes are divided by the number of averaged events: 22 000 for the signal II_{vf} kinetics and 35 000 for the oxygen release kinetics. The instrument time constant for oxygen release kinetics is 320 μs. Other conditions are as in Figure 1.

Scheme 1[a]

$$Y_Z + S_3 \xrightarrow[<1\mu s]{h\nu} Y_Z^{\bullet} + S_3 \xrightarrow{800-1400\mu s} Y_Z + (S_4) \xrightarrow{<50-200\mu s} Y_Z + S_0 + O_2\uparrow$$

Scheme 2

$$Y_Z + S_3 \xrightarrow[<1\mu s]{h\nu} Y_Z^{\bullet} + S_3 \rightarrow \boxed{\text{Molecular Rearrangement}} \xrightarrow{800-1400\mu s} Y_Z + S_0 + O_2$$

$$H^+ (?)$$
$$< 50\text{-}200\ \mu s$$

[a]Two possible reaction pathways for O_2 formation consistent with the O_2 release kinetics observed here. Scheme 2 is more consistent with the $Y_Z^{\bullet}$ turnover and electrochromic kinetics observed by Rappaport et al. (*29*).

DISCUSSION

These results give the first unequivocal demonstration that a kinetically identifiable transient is associated with the O_2 formation or release kinetics in PSII, following turnover from the S_3 state. Under conditions of essentially functional turnover, this transient may be as long 200 μs, but is <50 μs under optimal conditions. While this might represent simply a diffusion barrier to O_2 release into a region accessible to the tempone probe, this seems highly implausible given the known permeability of membranes to small neutral molecules (*26*), as well as the fact, demonstrated here, that modest pH changes modulate the effect by nearly an order of magnitude. This latter observation, in addition to the high ionic strength result (likely if anything to "loosen" the peripheral protein matrix around the OEC), argues for a chemical origin of the transient. Beyond the transient, however, the present data show clearly that the O_2 formation chemistry is closely coupled to the electron transfer responsible for $Y_z^{\bullet}$ rereduction following a flash turnover in the S_3 state, and that this is the rate-determining step.

It appears that at least two physically reasonable reaction sequences could accommodate our results. These are shown as Schemes 1 and 2. The first is the conventional ordering showing the formation of a transient S_4 state, which undergoes a 4 electron concerted reaction to produce O_2 from two water (or hydroxyl, or oxyl) groups. The resolved transient in our measurements would then define the lifetime of this state. However, because our measurement of the $Y_z^{\bullet}$ kinetics is basically a mixture of all S state contributions (with the lower S state components significantly attenuated due to the 40 μs time constant used), the *early* ($\leq$200 μs) time course of $Y_z^{\bullet}$ rereduction following the flash in S_3 is obscured somewhat. Thus it is possible that the lag reported by O_2 release represents actually a lag in $Y_z^{\bullet}$ rereduction, as in Scheme 2, and that no "formal" S_4 state exists. An important distinction between these reactions, apart from the obvious implications for the detailed O_2 formation chemistry, is that Scheme 1 requires 4 oxidizing equivalents to be stored (transiently) in the Mn cluster of the OEC, while Scheme 2 requires only 3. These storage requirements appear inescapable given the demonstration by Wydrzynski and colleagues (*27*) that substrate water is freely exchangeable with the OEC up to S_3.

A likely decision between the two reaction sequences is possible when optical absorbance data on Y_z turnover and electrochromism in the OEC are considered (*28*, *29*). These measurements typically have nearly an order of magnitude faster time resolution than our EPR data. Lavernge and colleagues found that when Y_z turnover was monitored at 295 nm, the $t_{1/2}$ for $Y_z^{\bullet}$ rereduction following turnover from S_3 was the same (1.2 ms) as that seen by us for PSII membranes under comparable conditions, but that an initial lag ($t_{1/2} \sim 30$ μs) preceded $Y_z^{\bullet}$ reduction. When viewed electrochromically (440−424 nm changes), the same transition showed a rapid initial change ($t_{1/2} \sim 30$ μs) followed by a slower change, with the latter decay kinetics indistinguishable from that of $Y_z^{\bullet}$ reduction ($t_{1/2} \sim 1.2$ ms). Our own extensively averaged data at 20 μs time resolution (*7*) on PSII membranes would seem to exclude any lag of order 50 μs in the $Y_z^{\bullet}$ rereduction kinetics for the Kok transitions up to S_3, but not for the $S_3 \rightarrow S_0$ transition, which within the uncertainty of the data might exhibit such an effect (see Figures 6 and 8 in ref *7*). Taken together, these results suggest that Scheme 2 is favored, that is, that the lag in O_2 release arises from a lag in $Y_z^{\bullet}$ rereduction on flashing the S_3 state. A definitive demonstration would involve a determination of the "pure" $S_3 \rightarrow\rightarrow S_0$ $Y_z^{\bullet}$ turnover of one of the perturbed samples, using a procedure such as that employed previously by us for thylakoids and PSII membranes (*6*, *7*). Unfortunately, the EPR S state synchronizing and measurement protocol necessary for such measurements places significant demands on the sample integrity and long term stability. So far, we have successfully used this procedure only with samples operating under optimum conditions. However, examination of Figures 1a, 2a, 3a, and 4a shows that *only* in Figure 3 does the fit of eqs 3 and 4 to the $Y_z^{\bullet}$ turnover response significantly fail to reproduce the data below 100 μs (by about 3σ of the noise), and this case corresponds of course to the instance of most pronounced initial lag in the O_2 release kinetics. Here the O_2 release delay is at least a

factor of 5 greater than under optimum control conditions, while the $Y_z^\bullet$ rereduction kinetics have been only modestly slowed (~30%) and the fraction of uncoupled centers (I_s component) is not significantly different from the control value.

The biphasic electrochromic response on the $S_3 \rightarrow \rightarrow S_0$ transition in PSII membranes has been interpreted (*29*) in terms of models similar to Scheme 2. The fast (30 μs) phase of the electrochromic response, as well as the equivalent $Y_z^\bullet$ rereduction lag, is suggested to arise from either proton ejection or OH^- binding in the vicinity of the electrochromic reporter (probably P_{680}), and this event "primes" the Mn cluster responsible for oxygen chemistry. This would then occur rapidly by a concerted four electron process, with one electron reducing $Y_z^\bullet$ *electrogenically*, and the other three reducing the Mn center(s). Since the 295 nm absorption kinetics report about equally on $Y_z^\bullet$ and OEC Mn reduction (*29*), the difference, if any, between the rates of OEC turnover and $Y_z^\bullet$ reduction is at present unresolvably small. Our findings support this picture, both kinetically and phenomenologically, in terms of the expected effect of external pH on the lag phase reaction. The nature of the putative molecular rearrangement in Scheme 2 is as yet unknown, but the weak pH dependence of various OEC parameters between pH 5.5 and 8 (*23*) argues strongly for proton ejection rather than OH^- binding. The trigger for this local proton displacement, which may not involve release to bulk solvent, is presumably electrostatic following Y_z oxidation. That Y_z turnover is at least apparently electrogenic, however, is probably a requirement for *any* plausible mechanism of water oxidation within the OEC, including the hydrogen abstraction models of OEC function currently suggested by Babcock, Britt, and collaborators (see for example refs *30*, *31*). Although these models propose a coupled proton/electron transfer from Mn center(s) within the OEC to $Y_z^\bullet$, a formally electroneutral process, the *distances* moved by the positive and negative charges are likely to be quite different. Thus the proton typically moves only ~1 Å across a hydrogen bond to the phenoxide oxygen of Y_z (e.g. (*31*), Figure 1), while the electron could displace its average position by ~10 Å, from a Mn center to the phenoxide ring. In terms of local electrostatic changes, this is virtually equivalent to the movement of the electron alone.

REFERENCES

1. Kok, B., Forbush, B., and McGolin, M. (1970) *Photochem. Photobiol. 11*, 457−475.
2. Debus, R. J., Barry, B. A., Sithole, I., Babcock, G. T., and McIntosh, L. (1988) *Biochemistry 27*, 9071−9074.
3. Metz, J. G., Nixon, P. J., Rögner, M., Brudvig, G. W., and Diner, B. A. (1989) *Biochemistry 28*, 6960−6969.
4. Warden, J. T., Balnkenship, R. E., and Sauer, K. (1976) *Biochim. Biophys. Acta 423*, 462−478.
5. Babcock, G. T., Blankenship, R. E., and Sauer, K. (1976) *FEBS Lett. 61*, 286−289.
6. Razeghifard, M. R., Klughammer, C., and Pace, R. J. (1997) *Biochemistry 36*, 86−92.
7. Razeghifard, M. R., and Pace, R. J. (1997) *Biochim. Biophys. Acta 1322*, 141−150.
8. Joliot, P., Hofnung, M., and Chabaud, R. (1966) *J. Chim. Phys. 63*, 1423−1441.
9. Sinclair, J., and Arnason, T. (1974) *Biochim. Biophys. Acta 368*, 393−400.
10. Etienne, A. L. (1968) *Biochim. Biophys. Acta 153*, 895−897.
11. Arnason, T., and Sinclair, J. (1976) *Biochim. Biophys. Acta 430*, 517−523.
12. Bouges-Bocquet, B. (1973) *Biochim. Biophys. Acta 292*, 772−785.
13. Jursinic, P., and Dennenburg, R. J. (1990) *Biochim. Biophys. Acta 1020*, 195−206.
14. Plijter, J. J., Aalbers, S., Barends, J.-P., Vos, M., and Van Gorkom, H. J. (1988) *Biochim. Biophys. Acta 935*, 299−311.
15. Meunier, P. C., and Popovic, R. (1991) *Photosynth. Res. 28*, 33−39.
16. Mauzerall, D. (1990) *Plant Physiol. 94*, 278−283.
17. Canaani, O., Malkin, S., and Mauzerall, D. (1988) *Proc. Natl. Acad. Sci. U.S.A. 85*, 4725−4729.
18. Lavergne, J. (1989) *Proc. Natl. Acad. Sci. U.S.A. 86*, 8768−8772.
19. Tang, X.-S., Moussavi, M., and Dismukes, G. C. (1991) *J. Am. Chem. Soc. 113*, 5914−5915.
20. Strzalka, K., Walczak, T., Sarna, T., and Swartz, M. (1990) *Arch. Biochim. Biophys. 281*, 312−318.
21. Porra, R. J., Thompson, W. A., and Kriedemann, P. E. (1989) *Biochim. Biophys. Acta 975*, 384−394.
22. Boska, M., Blough, N. V., and Sauer, K. (1985) *Biochim. Biophys. Acta 808*, 132−139.
23. Ahlbrink, R., Haumann, M., Cherepanov, D., Bögerhausen, O., Mulkidijanian, A., and Junge, W. (1998) *Biochemistry 37*, 1131−1142.
24. Boska, M., Sauer, K., Buttner, W., and Babcock, G. T. (1983) *Biochim. Biophys. Acta 722*, 327−330.
25. Reiman, S., Mathis, P., Conjeaud, H., and Stewart, A. (1981) *Biochim. Biophys. Acta 635*, 429−433.
26. Pace, R. J., and Chan, S. I. (1982) *J. Chem. Phys. 76*, 4241−4247.
27. Messinger, J., Badger, M., and Wydrynski, T. (1995) *Proc. Natl. Acad. Sci. U.S.A. 92*, 3209−3213.
28. Lavergne, J., and Junge, W. (1993) *Photosynth. Res. 38*, 279−296.
29. Rappaport, F., Blanchard-Desce, M., and Lavergne, J. (1994) *Biochim. Biophys. Acta 1184*, 178−192.
30. Gilchrist, M. L., Ball, J. A., Randall, D. W., and Britt, R. D. (1995) *Proc. Natl. Acad. Sci. U.S.A. 92*, 9545−9549.
31. Tommos, C., and Babcock, G. T. (1998) *Acc. Chem. Res. 31*, 18−25.

BI9811765